Improved Photovoltaic Performance of Si Nanowire Solar Cells Integrated with ZnSe Quantum Dots

ARTICLE *in* THE JOURNAL OF PHYSICAL CHEMISTRY C · JUNE 2012

Impact Factor: 4.77 · DOI: 10.1021/jp301683q

4 AUTHORS, INCLUDING:

Jung-Ho Lee
Hanyang University
138 PUBLICATIONS **1,503** CITATIONS
SEE PROFILE

Keya Zhou
Harbin Institute of Technology
48 PUBLICATIONS **255** CITATIONS
SEE PROFILE

THE JOURNAL OF PHYSICAL CHEMISTRY C

Article

pubs.acs.org/JPCC

Improved Photovoltaic Performance of Si Nanowire Solar Cells Integrated with ZnSe Quantum Dots

Jin-Young Jung,[†] Keya Zhou,[†] Jin Ho Bang,*[,‡] and Jung-Ho Lee*[,†]

[†]Department of Chemical Engineering and [‡]Department of Chemistry and Applied Chemistry, Hanyang University, 55 Hanyangdaehak-ro, Sangnok-gu, Ansan, Kyeonggi-do 426-791, Republic of Korea

Supporting Information

ABSTRACT: Introducing a ZnSe quantum dot (QD) layer over silicon nanowire (Si NW) solar cells considerably enhances external quantum efficiency (EQE) over broadband wavelengths. This is attributed to the combination of two major benefits of ZnSe QDs: superior light trapping and photon down-conversion. The integration of ZnSe QDs on the Si NW solar cell significantly reduces Fresnel reflection at the silicon/air interface because the refractive index of ZnSe QDs falls between those of Si and air. As a result, the refractive index mismatch at the interface can be alleviated. This decreases the Si NW length required for obtaining superior light absorption over 90%, which consequently leads to a substantial reduction in surface recombination loss. A remarkable enhancement of ~30% in EQE around the absorption maximum of ZnSe QDs reveals that photon down-conversion by ZnSe QDs significantly contributed to EQE enhancement in a short-wavelength region. Our Si NW/ZnSe QDs hybrid solar cell showed nearly 13% improvement in power conversion efficiency compared to that of a bare Si NW counterpart, highlighting the feasibility of thin-layered semiconductor nanoparticles as a booster for highly efficient Si solar cells.

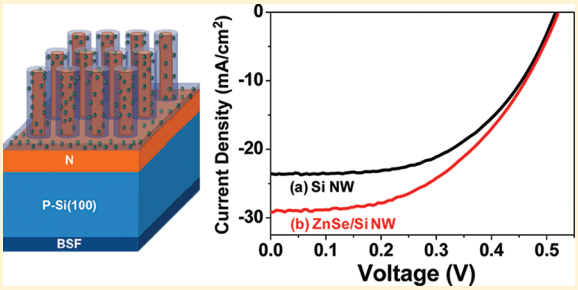

1. INTRODUCTION

Near-complete light absorptance throughout the whole solar spectrum is one of the vital factors for the development of next-generation silicon (Si) solar cells with high energy conversion efficiency and low production cost. Various surface texturing techniques have been devised for effective light absorption, including the fabrication of subwavelength Si nanowire (Si NW) arrays. This technique has recently attracted much interest due to its unique optical properties, such as excellent antireflection characteristics, efficient light trapping, and modulation of the optical bandgap.[1−4] Of the variety of nanostructured Si NWs, vertically aligned Si NW arrays hold great promise because they offer a superior broadband and omni-directional antireflectance. The distinctive optical characteristics of Si NW arrays arise from three light trapping mechanisms, including suppressed reflection via reduced mismatch in the refractive indexes of air and Si,[5−7] multiple scattering events within Si NW arrays,[8,9] and strong resonance in individual NWs by the antenna effect.[10,11]

Despite significant benefits from the one-dimensional Si nanostructure, the energy conversion efficiencies of Si NW solar cells are typically lower than those of their conventional Si counterparts, which is mainly due to high surface recombination loss.[12−15] In general, recombination loss depends on the length of Si NWs and constrains the energy conversion efficiency of Si NW solar cells. Si NW arrays with higher aspect ratios (i.e., long Si NWs) have high surface recombination velocity, leading to poor charge carrier collection efficiency.[14] In addition, conventional Si NW solar cells that form a planar bulk junction inside the wafer exhibit poor spectral responses, especially in a short-wavelength region. This feature is normally ascribed to the presence of a heavily doped thick emitter that acts as an electrically "dead layer" with high Auger recombination loss.[14,15] Given these adverse influences of the one-dimensional Si nanoarchitecture, a compromise is needed for the light absorptance and carrier collection efficiency of Si NW arrays. A strategy for enhancing light absorptance while avoiding serious deterioration in solar cell performance is of significant importance for developing highly efficient Si NW solar cells.

One approach to balancing these competing properties might be employing Si NWs with a lower aspect ratio (i.e., short Si NWs). Short Si NW arrays can enhance absorption through reasonable light trapping and are also less vulnerable to surface recombination than their longer counterparts. While this strategy is useful in promoting the energy conversion efficiency of Si NW solar cells,[16] the optical loss in short Si NW arrays is still significantly large. Nanoparticles with a high refractive index and a large bandgap have been proposed for use in antireflection layers.[17] The proper semiconductor nanoparticles (known as QDs) can compensate a mismatch in refractive indexes (n) at the interface between air (n = 1) and the silicon

Received: February 20, 2012
Revised: May 21, 2012
Published: May 23, 2012

   dx.doi.org/10.1021/jp301683q | J. Phys. Chem. C 2012, 116, 12409−12414

substrate (n = 3.42), leading to significant improvement in light absorption. Additional benefits of large bandgap QDs include the possibility of harvesting effective ultraviolet (UV) light emitted via photon down-conversion, a phenomenon in which an absorbed high-energy photon converts into two photons with lower energies.[18−22] High-energy photons corresponding to the UV part of the solar spectrum, which accounts for ∼7% of spectral irradiance, are generally not harnessed effectively by Si NWs. This is because the electron−hole pairs generated by UV illumination are readily switched into phonon scattering due to a high surface recombination rate. High-energy photons can be further harvested by the QDs being integrated on a Si solar cell and then converted into lower energy photons, a better route for photon collection.[20−22] Moreover, when QDs are coupled with a radial Si NW array, the additional enhancements of light absorption and charge carrier collection are possible due to the inherent physical properties of radial Si NW/QDs heterojunction.[23]

Here, we report an efficient approach for enhancing the energy conversion efficiency of Si NW solar cells by using ZnSe QDs. A thin layer of ZnSe QDs over Si NWs serves as an antireflection layer, which enables the fabrication of short-NW solar cells that alleviate surface recombination. The antireflectance of ZnSe QDs greatly improved light harvesting while reducing the NW lengths required for obtaining light absorption over 90%. ZnSe QDs also possess a bandgap of ∼3.1 eV, which is optimal for harvesting UV light. A remarkable enhancement (∼30%) in EQE near 400 nm revealed that photon down-conversion via ZnSe QDs also enhanced the conversion efficiency of Si NW solar cells. The hybrid solar cell utilizing Si NW/ZnSe QDs exhibited considerable enhancement in EQE over broadband wavelengths due to the combined effects of superior light trapping and photon down-conversion.

2. EXPERIMENTAL SECTION

2.1. Synthesis of Si NW Array. Vertically aligned Si NW arrays were prepared using metal-assisted electroless etching (MAE).[7,24] Silver (Ag) nanoparticles were first uniformly deposited onto a Si (100) substrate (p-type, 1−10 Ω·cm) by galvanic displacement in which the Si substrate was immersed into an aqueous solution of HF (4.8 M) and $AgNO_3$ (0.01 M) at 20 °C for 30 s. The Si substrate coated with Ag nanoparticles was washed and subsequently placed in an aqueous solution of HF (4.8 M) and H_2O_2 (0.5 M) at room temperature for 10 s to grow a Si NW array with a diameter of 50−200 nm. The lengths of Si NW arrays were adjusted by changing etching times. The Si substrate was then washed with concentrated nitric acid for 20 min to completely remove residual silver nanoparticles and dried under air. To form a bulk p−n junction underneath the Si nanowire array, phosphorus doping (P-doping) was performed using a spin-on-doping (SOD) technique. Phosphorus silicate precursors (P509, Filmtronics) were spin-coated on a dummy wafer, and the phosphorus-coated dummy wafer was placed near a target substrate (Si NW array) inside a tube furnace. The thin n^+ layer was formed via phosphorus diffusion at 870 °C for 5 min. The p-doping process was detailed in our previous work.[7] After creating the p−n junction, rapid thermal oxidation was followed by introducing dry oxygen gas into the furnace so as to form a thin SiO_2 layer not only for surface passivation[25] but also for preventing a possible degradation in electrical performances when ZnSe QD layer was directly deposited on top of a p−n junction.

2.2. Synthesis of ZnSe QDs. ZnSe QDs were synthesized via thermal decomposition of organometallic zinc and solvent-coordinated selenium, as reported previously.[26] Zinc stearate was dissolved in octadecene (ODE) containing octadecylamine (ODA) by heating up to 330 °C under a N_2 atmosphere. Selenium dissolved in trioctylphosphine (TOP) and ODE was quickly injected into this solution, and the temperature was held at 310 °C for 2 min to grow ZnSe QDs. After cooling down to room temperature, the ZnSe QDs were washed with a mixture of methanol and toluene and were dissolved in toluene for use.

2.3. Characterization. The reflection (R) and transmission (T) spectra of the Si NW array specimens were measured using a Perkin-Elmer Lambda 750 UV/vis/NIR spectrophotometer with an integrating sphere (Labsphere) in a wavelength range of 300−1200 nm, which corresponds to the major spectral irradiance of sunlight. The total absorption (A) spectra of each array was calculated using the equation $A = 1 - R - T$. Scanning electron microscopy (SEM) was performed using a field-emission scanning electron microscope (Hitachi S-4800 FESEM). Transmission electron microscopy (TEM) was carried out using a JEOL 2010F equipped with an EDS (energy dispersive X-ray spectroscopy) detector at an acceleration voltage of 200 kV. For device fabrication, the ZnSe QDs dispersed in toluene were drop-casted onto either planar Si substrate or the Si NW array (Scheme 1). A backside electrode was fabricated using the Ga/In eutectic, and Ag was deposited on the unetched planar region of the Si NW solar cells as a top electrode to exclude measurement variations caused by contact resistance (Figure S1 in Supporting Information). The total cell area measured is 0.5 cm^2. The photovoltaic performance of Si NW solar cells was investigated under the illumination of AM 1.5G (100 mW/cm^2) using a solar simulator (Peccel PEC-L11). EQE spectra were measured under calibrated, monochromatic light illumination obtained from a xenon light source equipped with a monochromator operating in the wavelength range of 300−1100 nm. The light intensity was calibrated with a silicon standard cell (PV Measurements, Inc.).

Scheme 1. Schematic Illustration of (a) Planar Si and (b) Si NW Solar Cells Integrated with ZnSe QDs

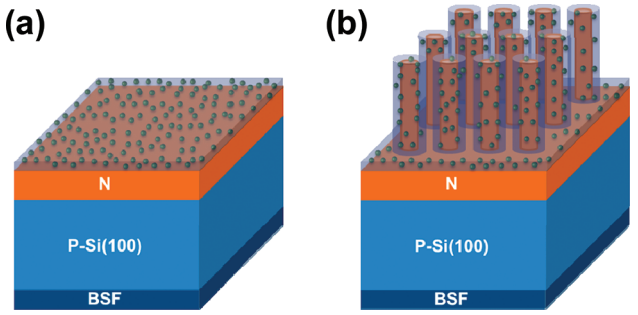

3. RESULTS AND DISCUSSION

The ZnSe QDs used in this study were prepared using conventional hot injection. The TEM image shown in Figure 1A combined with EDS analysis (Figure S2) reveals that the ZnSe QDs are nearly monodisperse and crystalline with an

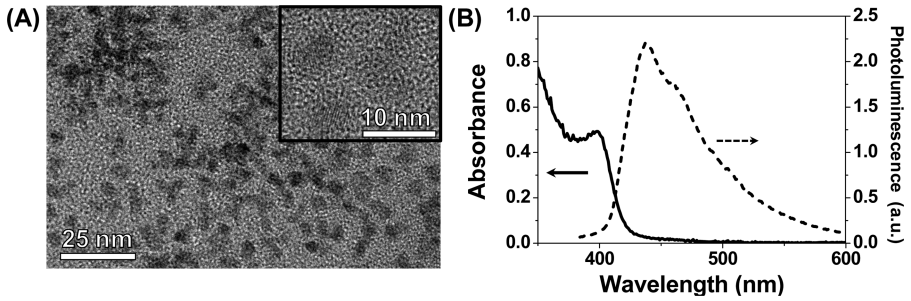

Figure 1. (A) TEM image of ZnSe QDs (inset: HRTEM image of ZnSe QDs). (B) UV−vis absorption and photoluminescence spectra of ZnSe QDs in toluene.

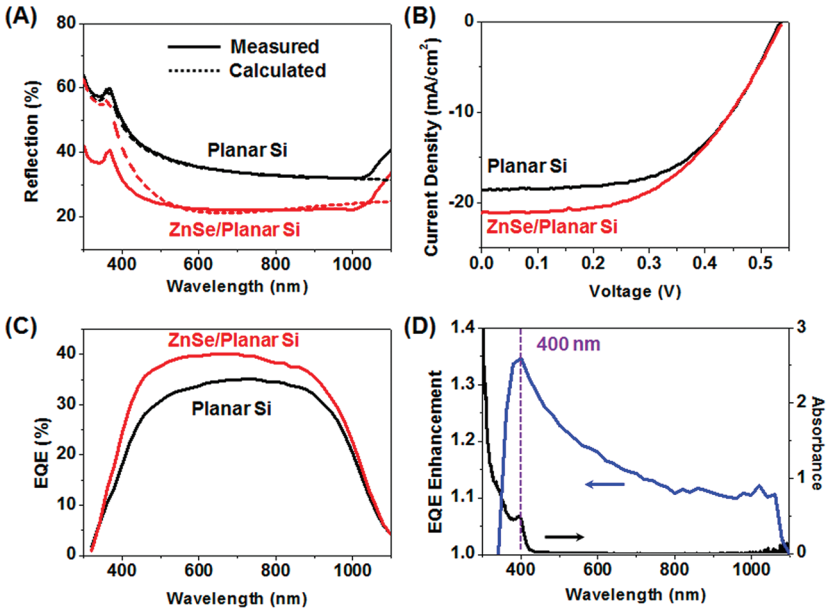

Figure 2. (A) Optical reflectance spectra (solid line: measured; dashed line: simulated), (B) $I-V$ characteristics, and (C) EQE spectra of a planar Si solar cell (black) and a planar Si solar cell integrated with ZnSe QD layer (red). (D) EQE enhancement of planar Si solar cell integrated with ZnSe QD layer in comparison with planar Si solar cell and absorption spectrum of ZnSe QDs.

average diameter of 6 nm. Figure 1B displays the absorption and photoluminescence spectra of ZnSe QDs. The ZnSe QDs exhibit typical absorption characteristics with a first excitonic peak at 398 nm. The band-edge emission is denoted along with a broad tailing feature down to ~600 nm, which stems mostly from the presence of trap states in ZnSe QDs triggered by surface defects.[27] Our optical analyses support that ZnSe QDs are attractive candidates for UV-to-visible conversions.

The usefulness of ZnSe QD layers for antireflection was first evaluated with planar Si solar cells. Figure 2A shows the reflectance spectra of planar Si solar cells integrated with and without a ZnSe QD layer. Polished, planar Si showed high average reflection of ~40% over the entire examined spectrum (300−1100 nm). However, integration of a 120 nm thick, ZnSe QD layer significantly suppressed light reflection to below 30%. The calculated effective refractive index (n_{eff}) for a ZnSe QD (coated with organic stabilizers) layer is 1.3, which can be acted as an optical buffer for impedance matching in effective refractive indexes between air and silicon substrate. Theoretical calculations of reflectance spectra have been performed using COMSOL Multiphysics simulation based essentially upon the thickness and effective refractive index of a ZnSe QDs layer. In long wavelengths above 500 nm, calculated results are matched well with the measured data because the antireflection for absorption enhancement stems mostly from the refractive index matching (see Figure S3). In wavelengths shorter than 500 nm, however, we could observe the mismatch between measured and calculated spectra, in which the reflectance in a spectrum measured for the QDs-coated-substrate depressed much remarkably compared to the simulated one. This discrepancy can be understood based on the two additional optical features typical in short wavelengths, i.e., light scattering enhanced by ZnSe QDs and their own light absorption for a frequency down conversion, but not considered for calculation. Light scattering by the ZnSe QD layer is dictated by Rayleigh scattering, which is validated by the condition of particle diameters such that $d \ll \lambda/(\pi n)$, where the n of ZnSe is 2.4. Scattering cross section (σ) depends critically on both particle diameter (d^6) and wavelength (λ^{-4}).[28] Note that σ is defined as the effective area of particles in a geometrical cross section for determining the probability of scattering events. In very small particles such as ZnSe QDs, scattering behavior is stronger in shorter wavelengths than in longer wavelengths because the scattering cross section is dictated by wavelength rather than by particle diameter. Such uneven light scattering is confirmed in the absorption enhancement spectra with a relative cross section of Rayleigh scattering (Figure S3).

dx.doi.org/10.1021/jp301683q | J. Phys. Chem. C 2012, 116, 12409−12414

The effect of ZnSe QD layer on solar cell performance was examined by measuring $I-V$ characteristics under AM 1.5G illumination (Figure 2B). The solar cell performance is summarized in Table 1. Integration of ZnSe QD layer increased

Table 1. Photovoltaic Performance of Si Solar Cells

	V_{oc} (mV)	J_{sc} (mA/cm^2)	FF (%)	PCE (%)
planar Si	528	18.75	55.5	5.50
ZnSe/planar Si	530	21.6	50.6	5.80
Si NWs (250 nm)	514	23.58	53.5	6.60
ZnSe/Si NWs (250 nm)	518	29.18	48.4	7.45
Si NWs (500 nm)	521	27.41	50.6	7.22
ZnSe/Si NWs (500 nm)	531	28.2	49.4	7.33

short-circuit current density (J_{sc}) from 18.7 to 21.6 mA/cm^2, reflecting a 15% enhancement compared to bare Si solar cells. However, there was no change in open-circuit voltage (V_{oc}) since the Fermi level was not affected by a ZnSe QD layer. Fill factor (FF) deteriorated slightly from 55.5 to 50.6% because the QD layer over the Si NWs increased series resistance. Nevertheless, the overall performance of planar solar cells was improved by integrating a ZnSe QD layer. This is largely due to J_{sc} enhancement, which stems from reduced light reflection due to the QD layer. This is also in good accordance with the EQE result that reflects improved conversion efficiencies over the entire spectrum (Figure 2C).

Besides their contribution to antireflection, ZnSe QDs were also evaluated in terms of photon down-conversion. As discussed earlier, high-energy photons absorbed by ZnSe QDs could be down-converted to low-energy photons, which can be more effectively converted to photocurrent. To verify the down-conversion effect of ZnSe QDs, the EQEs of Si solar cells with and without ZnSe QDs were compared. EQE enhancement is defined as a ratio between the EQEs with and without ZnSe QD layers at a given wavelength. Figure 2D shows that the EQE enhancement maximized at ~400 nm. This wavelength is consistent with a peak position of ZnSe QDs in our absorbance spectra, which strongly implies that ZnSe QDs aid in effectively harvesting UV light via photon down-conversion.

We demonstrated that the integration of ZnSe QDs onto planar Si solar cells enhanced their J_{sc} values due to the combined effects of better light trapping and photon down-conversion. Since the light reflection of a planar Si/ZnSe QDs solar cell is still higher than that of conventional, surface-textured solar cells, we tried to make further improvement by adopting a silicon nanostructured solar cell rather than a planar one. Si NW/ZnSe QDs hybrid solar cells were fabricated with the Si NWs (a wire filling ratio of 20%) prepared by MAE. Figure 3 shows a cross-sectional SEM image of the Si NW array before and after integration of ZnSe QDs. A ~50 nm thin, ZnSe QD layer uniformly covered the entire Si NW array. One-

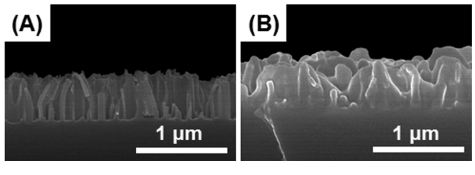

Figure 3. SEM image of Si NWs (A) before (B) after integration of ZnSe QD layer.

dimensional Si nanostructures were previously known to improve the optical responses of Si solar cells by increasing the wire length.[16] However, the poor collection efficiency of charge carriers due to enhanced recombination velocity readily counteracted the optical benefit in a short-wavelength region.[14,15] To effectively improve the conversion efficiency, the Si NW lengths were adjusted to find an optimal length upon integration with the ZnSe QD antireflection layer. As demonstrated with planar Si solar cells, the integration of ZnSe QD layer allows decreased Si NW lengths because it enhances antireflectance while avoiding serious degradation in carrier collection efficiency.

To evaluate the light absorptance of Si NW/ZnSe QD solar cells with the different wire lengths of 250 and 500 nm, optical reflectance spectra were compared before and after the integration of ZnSe QDs (Figure 4). Light reflection in both

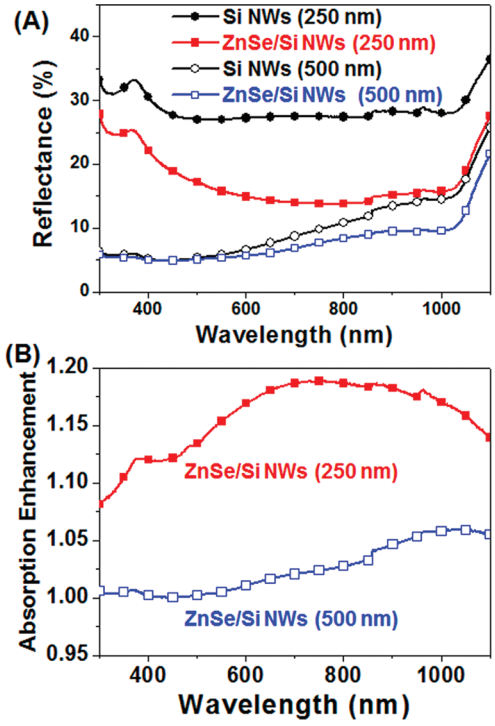

Figure 4. (A) Optical reflectance spectra of various Si NW solar cells; short Si NWs (250 nm), short Si NWs (250 nm) with QDs, long Si NWs (500 nm), and long Si NWs (500 nm) with QDs. (B) Absorption enhancement of Si NW solar cells with QDs; 250 nm (red) and 500 nm (blue) Si NW array.

cases significantly decreased in comparison to planar Si. This trend became more remarkable as wire lengths increased. The two distinctive features of multiple scattering and reduced refractive index mismatch accounted for the superior antireflection characteristics of the Si NW array.[29] Si NWs with an effective refractive index of 1.6 at 600 nm can be effective for optical impedance matching in refractive indexes between air (n = 1) and a silicon substrate (n = 3.94 at 600 nm). With integrated ZnSe QDs, the reflection in the NW samples also decreased as in planar Si. However, this tendency was more noticeable in a shorter NW (250 nm) than in a longer one (500 nm). The absorption enhancement caused by the ZnSe QD layer is more obvious in long-wavelength regions (Figure 4B). This contrasts with the planar case, in which absorption enhancement occurred in short-wavelength regions

dx.doi.org/10.1021/jp301683q | J. Phys. Chem. C 2012, 116, 12409−12414

below 400 nm. This behavior might be closely related to the optical confinement effect in the long-wavelength region, which is caused by hybridization of subwavelength-structured-Si NWs and ZnSe QDs in which the effective refractive index of core (Si NW)/shell (QDs) is nearly the same as that of bare NWs without QDs.

Si NW arrays that have a high refractive index with diameters larger than 100 nm can serve as cylindrical cavities.[30] This allows light to couple with Si NWs while generating resonant optical modes, such as guided and leaky modes, which can effectively trap, absorb, or scatter light at their optically resonant wavelengths. It has also been reported that a dielectric shell surrounding Si NWs significantly reinforced their optical confinement and caused their resonant wavelength to red-shift.[31] In our hybrid structure, the ZnSe QD layer surrounding Si NWs could also induce a similar optical confinement inside the Si NWs. This effect resulted in considerable improvement in light absorption of low-energy photons. The maximum absorption enhancement for wire lengths of 250 and 500 nm reached ~1.18 and ~1.05, respectively (Figure 4B). This result shows that the integration of ZnSe QDs more effectively enhances the light absorption in short Si NWs. We estimated that the Si NW/ZnSe QDs hybrid solar cell was capable of enhancing light absorptance through the two major effects of refractive index matching and optical confinement. These results show that Si NW/ZnSe QDs hybrid structures are promising in the development of next-generation Si solar cells that suffer from insufficient light absorption for low-energy photons.[32]

From the viewpoint of the optical responses, a longer NW array (500 nm) is expected to be more efficient than a short one (250 nm). In fact, improved light absorption increased the J_{sc} of Si NW solar cells without QDs (Figure 5A) so that a long one showed better performance than its short counterpart (Table 1). However, we need to note that the overall solar cell performance was further improved on the integration of a ZnSe QD layer, in which the short NW array was found to perform better than the long one (Table 1). If we further increase the NW length up to 1 μm, the overall cell performances became worse than that of 500 nm NW array irrespective of a QD layer, which affirms that too long Si NW arrays suffer greatly from a high surface recombination velocity (Figure 5B).

These results led us to focus on the trade-off relationship between enhancement in light absorption and degradation in surface and Auger recombination when applying one-dimensional Si nanostructures for solar cell fabrication. The EQE data shown in Figure 6A also clarifies this feature. While light absorption is much better for long NWs over broad wavelengths (300−1100 nm), EQEs in the short-wavelength region of 300−600 nm are notably degraded in long wires. As wire length increases, recombination losses are known to occur by the two major routes of surface and Auger recombinations. Since most high-energy photons are absorbed near the surface of wires, recombination loss is dramatic in a short-wavelength region. Given our optical results, a short NW array would be the preferred option for highly efficient Si solar cells that minimize recombination loss with reasonable light absorbance. The integration of ZnSe QDs significantly enhances the light absorption without the degradation of carrier collection efficiency in the short-wavelength region, which enables us to obtain the highest J_{sc} value with the short Si NW (250 nm).

In short NW samples, a sudden depression in EQE was not observed near the UV region despite great increases in surface

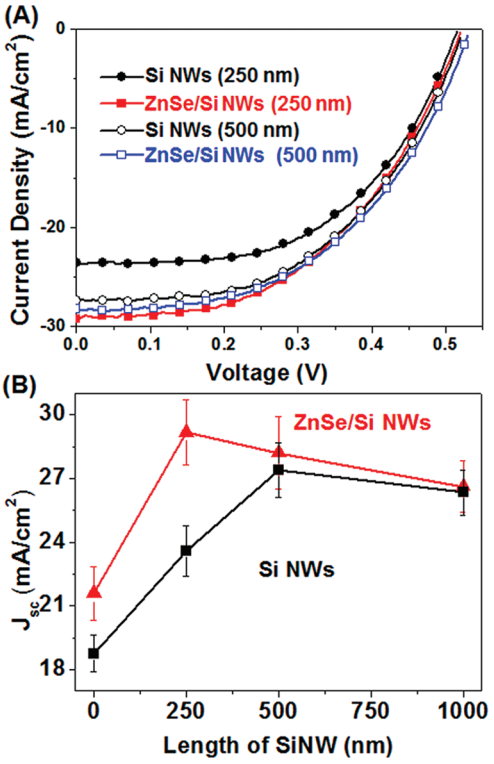

Figure 5. (A) $I-V$ characteristics of various Si NW solar cells; short Si NWs (250 nm), short Si NWs (250 nm) with QDs, long Si NWs (500 nm), and long Si NWs (500 nm) with QDs. (B) Comparison of J_{sc} for Si NW solar cells.

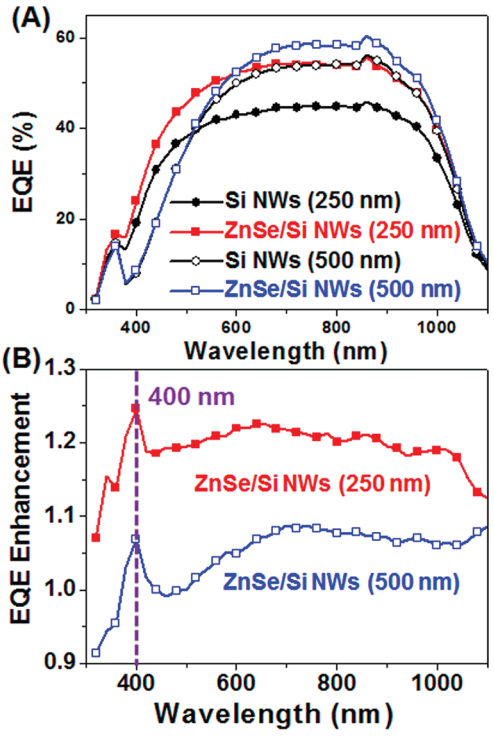

Figure 6. (A) EQE spectra of Si NW solar cells; short Si NWs (250 nm), short Si NWs (250 nm) with QDs, long Si NWs (500 nm), and long Si NWs (500 nm) with QDs. (B) EQE enhancement of Si NW solar cells integrated with ZnSe QDs; 250 nm (red) and 500 nm (blue) Si NW array.

dx.doi.org/10.1021/jp301683q | J. Phys. Chem. C 2012, 116, 12409−12414

area due to the wired topology. In fact, the EQE spectra obtained were similar to those of planar Si. This observation suggests the possibility of a short-NW solar cell for enhancing light absorption without serious degradations in carrier collection. A substantial improvement in EQE stems mainly from improved light trapping and photon down-conversion. The photon down-conversion effect is confirmed by Figure 6B, which shows the peak of EQE enhancement at the absorption of ZnSe QDs. The EQE enhancement of 1.25 at 400 nm which is larger than the absorption enhancement of 1.12 implies that the frequency down-shifted photons might contribute to additional ~10% improvement in a conversion efficiency.

4. CONCLUSIONS

An effective method for improving the conversion efficiency of Si NW solar cells based upon the optical effect of ZnSe QDs was demonstrated. A Si NW/ZnSe QDs hybrid solar cell showed considerable enhancement in EQE over broadband wavelengths due to light trapping and photon down-conversion. The superior antireflection characteristics of ZnSe QDs significantly improved light absorption, which decreased the optimized NW length required for achieving efficient light absorptance. A short Si NW array of 250 nm could enhance solar cell performance while avoiding an EQE depression due to surface recombination of photogenerated carriers at the UV range. EQE enhancement maximized at the wavelength where light absorption by ZnSe QDs was the largest. This result affirms that photon down-conversion by ZnSe QDs contributed to efficiency enhancement as well. Further improvement could be achieved by optimizing the integration condition of the Si NW/ZnSe QDs solar cell. The strategy presented in this work would open up new opportunities for developing highly efficient next-generation solar cells.

■ ASSOCIATED CONTENT

Ⓢ Supporting Information

Schematic illustration for measurement setup; TEM-EDS analysis of ZnSe QDs; absorption enhancement of planar Si/ZnSe QDs hybrid solar cell. This material is available free of charge via the Internet at http://pubs.acs.org.

■ AUTHOR INFORMATION

Corresponding Author

*E-mail: jungho@hanyang.ac.kr (J.-H.L.); jbang@hanyang.ac.kr (J.H.B.).

Notes

The authors declare no competing financial interest.

■ ACKNOWLEDGMENTS

This work was supported by the Pioneer Research Center Program through the National Research Foundation of Korea (NRF, No. 2011-0001646) and by the NRF grant (No. 2011-0028604) funded by the Ministry of Education, Science, and Technology (MEST). This work was also supported by the Human Resources Development of the Korea Institute of Energy Technology Evaluation and Planning (KETEP) grant funded by the Ministry of Knowledge Economy, Republic of Korea (No. 20104010100620).

■ REFERENCES

(1) Chang, H. C.; Lai, K. Y.; Dai, Y. A.; Wang, H. H.; Lin, C. A.; He, J. H. *Energy Environ. Sci.* **2011**, *4*, 2863−2869.
(2) Hu, L.; Chen, G. *Nano Lett.* **2007**, *7*, 3249−3252.
(3) Diedenhofen, S. L.; Janssen, O. T. A.; Grzela, G.; Bakkers, E. P. A. M.; Rivas, J. G. *ACS Nano* **2011**, *5*, 2316−2323.
(4) Jung, J.-Y.; Zhou, K.; Um, H.-D.; Guo, Z.; Jee, S.-W.; Park, K.-T.; Lee, J.-H. *Opt. Lett.* **2011**, *36*, 2677−2679.
(5) Diedenhofen, S. L.; Vecchi, G.; Algra, R. E.; Hartsuiker, A.; Muskens, O. L.; Immink, G.; Bakkers, E. P. A. M.; Vos, W. L.; Rivas, J. G. *Adv. Mater.* **2009**, *21*, 973−978.
(6) Zhu, J.; Yu, Z. F.; Burkhard, G. F.; Hsu, C. M.; Connor, S. T.; Xu, Y. Q.; Wang, Q.; McGehee, M.; Fan, S. H.; Cui, Y. *Nano Lett.* **2009**, *9*, 279−282.
(7) Jung, J.-Y.; Guo, Z.; Jee, S.-W.; Um, H.-D.; Park, K.-T.; Lee, J.-H. *Opt. Express* **2010**, *18*, A286−A292.
(8) Muskens, O. L.; Rivas, J. G.; Algra, R. E.; Bakkers, E. P. A. M.; Lagendijk, A. *Nano Lett.* **2008**, *8*, 2638−2642.
(9) Street, R. A.; Wong, W. S.; Paulson, C. *Nano Lett.* **2009**, *9*, 3494−3497.
(10) Cao, L. Y.; White, J. S.; Park, J. S.; Schuller, J. A.; Clemens, B. M.; Brongersma, M. L. *Nat. Mater.* **2009**, *8*, 643−647.
(11) Cao, L. Y.; Fan, P. Y.; Vasudev, A. P.; White, J. S.; Yu, Z. F.; Cai, W. S.; Schuller, J. A.; Fan, S. H.; Brongersma, M. L. *Nano Lett.* **2010**, *10*, 439−445.
(12) Dan, Y. P.; Seo, K.; Takei, K.; Meza, J. H.; Javey, A.; Crozier, K. B. *Nano Lett.* **2011**, *11*, 2527−2532.
(13) Jung, Y. W.; Vacic, A.; Perea, D. E.; Picraux, S. T.; Reed, M. A. *Adv. Mater.* **2011**, *23*, 4306−4311.
(14) Li, H. F.; Jia, R.; Chen, C.; Xing, Z.; Ding, W. C.; Meng, Y. L.; Wu, D. Q.; Liu, X. Y.; Ye, T. C. *Appl. Phys. Lett.* **2011**, *98*, 151116.
(15) Toor, F.; Branz, H. M.; Page, M. R.; Jones, K. M.; Yuan, H. C. *Appl. Phys. Lett.* **2011**, *99*, 103501.
(16) Huang, B.-R.; Yang, Y.-K.; Lin, T.-C.; Yang, W.-L. *Sol. Energy. Mater. Sol. Cells* **2012**, *98*, 357−362.
(17) Wan, D.; Chen, H.-L.; Tseng, T.-C.; Fang, C.-Y.; Lai, Y.-S.; Yeh, F.-Y. *Adv. Funct. Mater.* **2010**, *20*, 3064.
(18) Richards, B. S. *Sol. Energy Mater. Sol. Cells* **2006**, *90*, 1189−1207.
(19) Aarts, L.; van der Ende, B.; Reid, M. F.; Meijerink, A. *Spectrosc. Lett.* **2010**, *43*, 373−381.
(20) Huang, C. Y.; Wang, D. Y.; Wang, C. H.; Chen, Y. T.; Wang, Y. T.; Jiang, Y. T.; Yang, Y. J.; Chen, C. C.; Chen, Y. F. *ACS Nano* **2010**, *4*, 5849−5854.
(21) Chen, H. C.; Lin, C. C.; Han, H. W.; Tsai, Y. L.; Chang, C. H.; Wang, H. W.; Tsai, M. A.; Kuo, H. C.; Yu, P. C. *Opt. Express* **2011**, *19*, A1141−A1147.
(22) Pi, X. D.; Li, Q.; Li, D. S.; Yang, D. R. *Sol. Energy. Mater. Sol. Cells* **2011**, *95*, 2941−2945.
(23) Song, T.; Zhang, F. T.; Lei, X. F.; Xu, Y. L.; Lee, S.; Sun, B. Q. *Nanoscale* **2012**, *4*, 1336−1445.
(24) Peng, K. Q.; Xu, Y.; Wu, Y.; Yan, Y. J.; Lee, S. T.; Zhu, J. *Small* **2005**, *1*, 1062−1067.
(25) Shen, X. J.; Sun, B. Q.; Liu, D.; Lee, S. T. *J. Am. Chem. Soc.* **2011**, *133*, 19408−19415.
(26) Lin, S. L.; Pradhan, N.; Wang, Y. J.; Peng, X. G. *Nano Lett.* **2004**, *4*, 2261−2264.
(27) Zhao, Y. W.; Zhang, Y.; Zhu, H.; Hadjipianayis, G. C.; Xiao, J. Q. *J. Am. Chem. Soc.* **2004**, *126*, 6874−6875.
(28) Akimov, Y. A.; Koh, W. S.; Sian, S. Y.; Ren, S. *Appl. Phys. Lett.* **2010**, *96*, 073111.
(29) Tsakalakos, L.; Balch, J.; Fronheiser, J.; Shih, M. Y.; LeBoeuf, S. F.; Pietrzykowski, M.; Codella, P. J.; Korevaar, B. A.; Sulima, O.; Rand, J.; et al. *J. Nanophotonics* **2007**, *1*, 013552.
(30) Cao, L. Y.; Fan, P. Y.; Barnard, E. S.; Brown, A. M.; Brongersma, M. L. *Nano Lett.* **2010**, *10*, 2649−2654.
(31) Liu, W. F.; Oh, J. I.; Shen, W. Z. *IEEE Electron Device Lett.* **2011**, *32*, 45−47.
(32) Green, M. A.; Basore, P. A.; Chang, N.; Clugston, D.; Egan, R.; Evans, R.; Hogg, D.; Jarnason, S.; Keevers, M.; Lasswell, P.; et al. *Sol. Energy* **2004**, *77*, 857−863.